

Reliability assessment for Modular Multilevel Converters using Monte Carlo Simulations

Ahmadi, Miad; Shekhar, Aditya; Bauer, Pavol

DOI

[10.1016/j.ijepes.2025.110482](https://doi.org/10.1016/j.ijepes.2025.110482)

Publication date

2025

Document Version

Final published version

Published in

International Journal of Electrical Power and Energy Systems

Citation (APA)

Ahmadi, M., Shekhar, A., & Bauer, P. (2025). Reliability assessment for Modular Multilevel Converters using Monte Carlo Simulations. *International Journal of Electrical Power and Energy Systems*, 165, Article 110482. <https://doi.org/10.1016/j.ijepes.2025.110482>

Important note

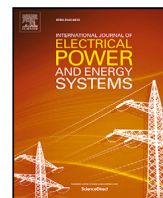
To cite this publication, please use the final published version (if applicable).
Please check the document version above.

Copyright



Other than for strictly personal use, it is not permitted to download, forward or distribute the text or part of it, without the consent of the author(s) and/or copyright holder(s), unless the work is under an open content license such as Creative Commons.

Takedown policy

Please contact us and provide details if you believe this document breaches copyrights.
We will remove access to the work immediately and investigate your claim.



Reliability assessment for Modular Multilevel Converters using Monte Carlo Simulations

Miad Ahmadi *, Aditya Shekhar , Pavol Bauer

Technische Universiteit Delft (TU Delft), Electrical Sustainable Energy Department, Mekelweg 4, Delft, 2628 CD, The Netherlands

ARTICLE INFO

Keywords:

Monte Carlo Simulation
Computation time
Modular Multilevel Converter
Redundancy methodologies
Reliability
Mission profile
MIL

ABSTRACT

Modular Multilevel Converters (MMCs) offer significant advantages in the medium to high-voltage settings. The modular architecture of MMCs allows for redundant submodules (SMs) to improve overall reliability. These redundant SMs can be deployed using various redundancy strategies, such as Load-Sharing Active Redundancy Strategy (LS-ARS), Fixed-Level Active Redundancy Strategy (FL-ARS), and Standby Redundancy Strategy (SRS). The primary contribution of this paper is the introduction of guidelines for applying Monte Carlo Simulation (MCS) and a comprehensive methodology for its application across various redundancy strategies. This enables precise planning of preventive maintenance and estimation of the number of faulty SMs with a specific lifespan in the MMC. More importantly, MCS is applied to estimate the reliability of the MMC applying Mission Profile for SRS and LS-ARS where analytical solutions are unavailable. An analysis of uncertainty and the applicability of MCS is also presented to demonstrate the advantages of MCS over analytical methods. The computational time required for applying MCS across different redundancy strategies and arm levels is also assessed.

1. Introduction

Reliability is a crucial factor in the design of Modular Multilevel Converters (MMCs) [1]. Component failures within the MMC can lead to significant impacts in terms of cost and overall system safety [2]. Hence, it becomes imperative to evaluate MMC reliability during the design and development phase [3]. To enhance the reliability of grid-connected MMC systems, modularity, redundancy, and reconfigurability are explored, as detailed in [4,5]. Various methodologies are employed to assess MMC reliability, including the mission profile method and statistical analysis. The mission profile method is rooted in the physics of a specific failure mechanism, focusing on time-to-failure or cycle-to-failure within the system's mission profile [6]. The latter methodology involves analytical formulations, utilizing standards such as the FIDES Guide and Military Handbook (MIL-HDBK) [7] to gauge system reliability [8]. Another valuable tool for reliability analysis is Monte Carlo Simulation (MCS), which is useful in considering the uncertainty of reliability indices [1,9]. MCS converges to a specific value as the number of trials increases, settling within the tolerance level range [10].

This study employs MCS tailored for MMCs, focusing on redundancy strategies and preventive maintenance planning. The following approaches are implemented:

1. Reliability Block Diagram (RBD): The RBD framework is utilized to model the success criteria of MMC arms under various redundancy strategies. For instance, in the Fixed-Level Active Redundancy Strategy (FL-ARS), reliability is calculated using the k -out-of- n probability model, where the system operates successfully if a minimum number of SMs remains functional. Similarly, the Standby Redundancy Strategy (SRS) assumes a homogeneous Poisson process to model the activation of spare SMs as failures occur [11].

2. MCS: MCS is employed in non-sequential and sequential forms to address the limitations of analytical methods, especially for complex scenarios like Load-Sharing Active Redundancy Strategy (LS-ARS). Sequential MCS allows the incorporation of time-dependent failure mechanisms, enabling precise planning of maintenance intervals and reliability estimation over the MMC's lifespan. This is particularly crucial for mission profile applications, where analytical solutions are unavailable [11].

3. Mission profile-based reliability assessment: To estimate lifetime reliability, the mission profile method integrates component degradation data, such as thermal stress and switching cycles. Combined with MCS, this method accounts for stochastic variations in operational conditions, providing a more accurate reliability estimate than traditional analytical approaches [12].

* Corresponding author.

E-mail address: m.ahmadi-3@tudelft.nl (M. Ahmadi).

These methodologies collectively enable a comprehensive assessment of MMC reliability, addressing practical challenges like redundancy allocation, and preventive maintenance planning.

MCS finds diverse applications, serving as both a validation tool and a means to account for parameter variations. In the context of [13], MCS is employed to validate theoretical outputs. The study demonstrates that with 10,000 trials, MCS outputs align closely with analytical results over a 40-year lifespan. However, specific details regarding the implementation of MCS are not provided.

The dynamic preventive maintenance strategy in [14] optimizes MMC reliability and maintenance costs by considering multi-term thermal cycles and operational conditions. It adjusts maintenance intervals dynamically to balance costs and reliability effectively. Authors in [15] introduced a Mixed Redundancy Strategy that combines active and spare redundant SMs to enhance system reliability, achieving over a 50% increase in B10 lifetime compared to traditional strategies. In [16], the authors focus on estimating the reliability of the DC/DC converter due to electrothermal stresses on power electronic switches and capacitors. The MCS accounts for variations in defined parameters. Authors in [17] developed a reliability model for MMC-based flexible interconnection controllers, accounting for current loading uncertainties and utilizing MCSs to refine the IGBT module's reliability assessment. The study reveals that introducing redundancy in such a converter can extend its lifetime from 4.5 to 7.5 years. Another instance of MCS application is highlighted in [18], where vehicle behavior is simulated to compare the service capacities and earnings of electric vehicle (EV) charging and battery swapping. This paper models the stochastic behavior of elements using MCS.

In [19], a mission profile-based reliability prediction method for MMCs, incorporating key modeling steps such as analytical power loss models, thermal modeling, lifetime modeling, Monte Carlo analysis, and redundancy analysis. In [20], three distinct MCS methods — static, semi-dynamic, and dynamic MCSs — are introduced to evaluate the reliability of power electronics based on the mission profile. However, MCS is primarily utilized to account for variations in applied parameters. The study reveals that the static MCS exhibits the fastest calculation time. From an accuracy perspective, it is concluded that if the number of trials exceeds 1000, there is no discernible difference among the outputs of various MCS strategies. Authors in [21] evaluated the lifetime of medium-voltage drives based on MMCs using Monte Carlo simulations, highlighting potential underestimations in traditional lifetime assessments. In [8], MCS is employed to investigate the reliability of a photovoltaic (PV) power plant. The study derives an estimation of failure rates from FIDES Guide standards, utilizing MCS to obtain the probability of system failure. Moreover, in [22,23], a reliability-based design method is proposed for MMC. MCS is applied to consider a 5% variation in applied parameters by acknowledging potential deviations in statistical analysis from actual values.

This paper aims to establish a guideline for applying MCS as a methodology for evaluating the reliability of MMC across various redundancy strategies. MCS provides the flexibility to account for improbable system effects that may not be captured by analytical approaches [24]. It is worth noting that this study does not prioritize a specific reliability methodology (MIL, FIDES, or mission profile) for measuring component failure rates. Nevertheless, MCS is a valuable and highly accurate tool for estimating the converter's failure rate. Unlike much of the existing literature, which primarily focuses on parameter deviation [25], this study broadens the scope of MCS application [26]. The key contributions of this study are summarized as follows:

- Propose the approach for applying MCS to assess the reliability of the MMC employing all available redundancy strategies, as detailed in Section 3.
- Compare the MCS outputs with analytical equations to validate the effectiveness of applying MCS (Section 3/2).

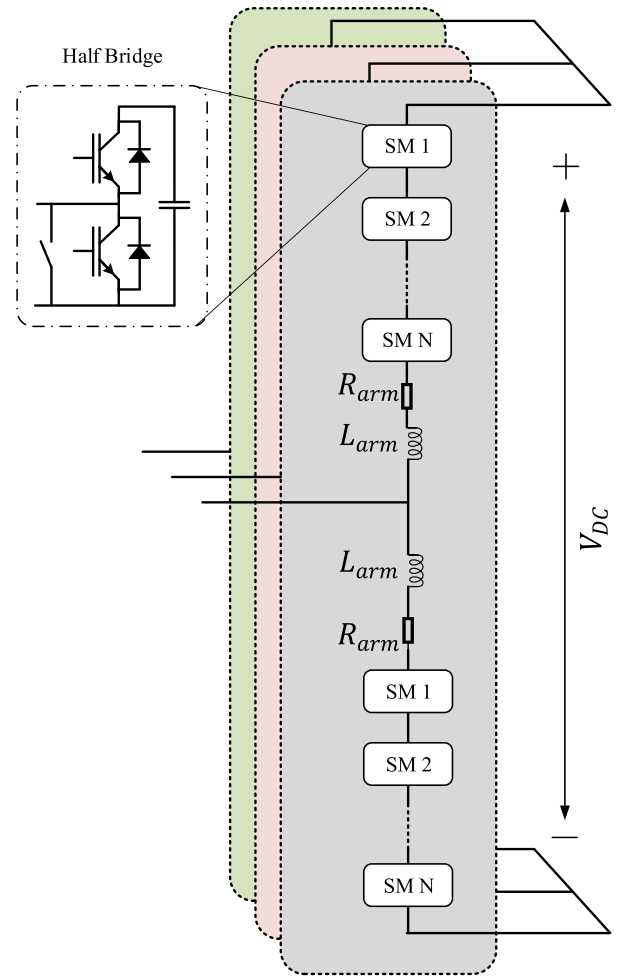


Fig. 1. Configuration of an MMC with half bridge SMs.

- Estimating the MMC's reliability by applying the mission profile method where the results are unavailable with two redundancy strategies (Section 4).
- Demonstrating the application of MCS in dynamic preventive maintenance (Section 4).
- Compute the required time for performing MCS with different system configurations (Section 5).

2. Redundancy strategies of MMC

The MMC configuration is depicted in Fig. 1, featuring three phases, each comprising two arms with Sub-Modules (SMs) connected in series to attain the desired voltage and power rating. As shown in Fig. 1, each SM includes an IGBT module, capacitor bank, and auxiliary components [27]. The minimum series connection of SMs required is dictated by the necessary DC-link voltage (V_{dc}) and the IGBT rating, as outlined in (1) [28,29].

$$N_{\min} = \text{Ceil} \left[\frac{k_{\max} \times V_{dc}}{S_f \times V_{IGBT}} \right] \quad (1)$$

here, S_f represents the safety factor for employing IGBT, and k_{\max} signifies the voltage ripple across the capacitors in the SM. To improve the reliability of the MMC and extend its availability time, additional SMs are employed, thereby enhancing reliability [30]. The integration of redundant SMs can be realized through various methods, outlined as follows:

2.1. FL-ARS

In the FL-ARS, also known as hot-reserved redundancy, only N_{\min} SMs operate actively, while redundant SMs remain powered and operational. However, the triggering signal in FL-ARS is specifically directed to N_{\min} randomly selected SMs. Consequently, all SMs take turns being triggered and operating, whether they are part of the original SMs or redundant SMs. It is important to note that in this redundancy strategy, all SMs experience constant voltage stress throughout MMC operation. The reliability of an arm in FL-ARS, as per the Reliability Block Diagram (RBD) model presented in [31], is determined using the k-out-of-n probability model, where the success of the arm requires N_{\min} SMs out of n SMs, where n is the total number of SMs in each arm, including redundant ones ($N_{\min} + N_{\text{red}}$). In the FL-ARS, the reliability of an arm is expressed by (2).

$$R_{\text{arm-FL}}(t) = \sum_{i=N_{\min}}^n C_n^i R_{\text{SM}}(t)^i (1 - R_{\text{SM}}(t))^{n-i} \quad (2)$$

$$R_{\text{SM}}(t) = e^{-\lambda_{\text{SM}} t} \quad (3)$$

where R_{SM} denotes the reliability of the SM, λ_{SM} represents the total failure rate of the SM, encompassing power switches, capacitor banks, power supply, gate drive, and thyristor. It is crucial to note that the failure rates of these components could be determined through various reliability methods. However, this study does not delve into calculating these specific failure rates or selecting components for consideration, as outlined in [32]. This study assumes these factors have been established and the associated failure rates are estimated with acceptable accuracy.

2.2. SRS

In the SRS, also known as cold-reserved redundancy, the operational SMs consistently number N_{\min} , while the redundant SMs remain idle. If an SM experiences a failure, the faulty SM is bypassed, and the first redundant SM is activated. Since the redundant SMs are bypassed in SRS, their failure rate is assumed to be zero. Like FL-ARS, the voltage stress across operational SMs is comparable in SRS. The reliability of an arm in SRS is determined using the Homogeneous Poisson Process with a failure rate of λ_s , where N_{\min} represents the minimum required number of SMs per arm. The reliability of an arm follows the Poisson Distribution, as expressed in (4) and (5), based on the RBD model outlined in [13].

$$R_{\text{arm-SRS}}(t) = P[N(t) \leq (n - N_{\min})] = \sum_{i=0}^{n-N_{\min}} \frac{(\lambda_s t)^i}{i!} e^{-\lambda_s t} \quad (4)$$

$$\lambda_s = \lambda_{\text{SM}} \times N_{\min} \quad (5)$$

2.3. LS-ARS

In the LS-ARS, the N_{red} redundant SMs are operational, and the load is distributed among $N_{\min} + N_{\text{red}}$ SMs. As a result, the operating voltage of each SM is lower in LS-ARS compared to SRS and FL-ARS. This reduction in operating voltage subsequently decreases the voltage stress and the SM failure rate. However, in the event of an SM failure, the voltage across the remaining SMs increases, which needs to be considered in the reliability evaluation.

$$\begin{aligned} P_0(t) &= e^{-n\lambda_{\text{SM}} t} \\ &\vdots \\ P_j(t) &= \int_0^t (n-j-1)\lambda_{\text{SM},n-j-1} e^{-(n-j)\lambda_{\text{SM},n-j} \tau} P_{j-1}(t-\tau) d\tau \\ &\vdots \\ P_{n-N_{\min}+1}(t) &= \int_0^t N_{\min} \lambda_{\text{SM},n-N_{\min}} P_{n-N_{\min}}(\tau) d\tau \end{aligned} \quad (6)$$

LS-ARS's RBD is presented in [33] and is not repeated here. Markov Chain (MC) is the method used to evaluate the MMC's reliability if the redundancy strategy is LS-ARS. In MC, state 0 corresponds to the initial state where all the SMs are operational and share the load. The fail state is presented as $n-N_{\min}+1$ where more than N_{red} SMs have failed. The equations obtained by the MC are as (6). Therefore, achieving effective arm operation involves combining successful states given by (7).

$$R_{\text{arm-LS}}(t) = \sum_{j=0}^{N_{\text{red}}} P_j(t). \quad (7)$$

After assessing the arm's dependability through the analysis of redundancy strategies, the reliability of the MMC can be computed using (8):

$$R_{\text{MMC-x}}(t) = R_{\text{arm-x}}(t)^6 \rightarrow x \in \text{FL-ARS, SRS, LS-ARS} \quad (8)$$

The failure rate in SRS is lower than FL-ARS, which is incorporated in the Poisson and k-out-of-n analytical methods used for these redundancy strategies, respectively. On the other hand, the failure rate for LS-ARS varies due to changes in voltage stress, which is incorporated using the Markov Chain method. The differences are also included to develop unique MCS method for each redundancy strategy and validated using the analytical methods, as described in Section 3.

3. Monte Carlo models of MMC under various redundancy strategies

MCS is a tool that assesses the reliability of a system by simulating its realistic functions and random behaviors. In MCS, a series of experiments (trials) are conducted to estimate the probability of system failure or success. In contrast, analytical approaches describe the system using mathematical equations, which are sometimes simplified.

There are two methods of applying MCS: time-independent (random) and time-dependent (sequential). The selected approach depends on the characteristics of the system. If the time intervals in MCS impact the subsequent intervals, time-dependent MCS should be employed. In time-dependent MCS, uniform numbers between 0–1 should be converted into the time distribution. As shown in (3), the exponential distribution can be transformed using the inverse transform method, outlined as follows [11]:

$$R_{\text{SM}}(t) = e^{-\lambda_{\text{SM}} t}, (\lambda_{\text{SM}} > 0, t \geq 0) \quad (9)$$

so the unreliability function can be obtained as (10).

$$U_{\text{SM}}(t) = 1 - R_{\text{SM}}(t) \rightarrow e^{-\lambda_{\text{SM}} t} = 1 - U_{\text{SM}}(t) \quad (10)$$

by applying the inverse transform function:

$$t = -\frac{1}{\lambda_{\text{SM}}} \ln(1 - U_{\text{SM}}(t)) \quad (11)$$

where $1 - U_{\text{SM}}(t)$ is uniformly distributed over the interval [0, 1]. Therefore, the time interval distribution for each SM can be determined. It is crucial to emphasize that even if the failure rate of the SM is estimated using the Weibull Distribution, which considers the wear-out period and component degradation in the mission profile reliability method, MCS remains applicable. However, when considering the wear-out period, the inverse transform function for MCS can be derived, as expressed in (12).

$$t = \eta \times \sqrt[\eta]{-\ln(1 - U_{\text{SM}}(t))} \quad (12)$$

where $1 - U_{\text{SM}}(t)$ is uniformly distributed over the interval [0, 1], with β and η representing the shape and scale parameters derived from the mission profile results. This will be more elaborated in Section 4 A. Throughout the remainder of this study, the methodology applied for MCS is demonstrated based on a single trial and by applying the failure rate achieved according to the MIL method. Nevertheless, the same method applies to mission profiles. However, it is imperative to

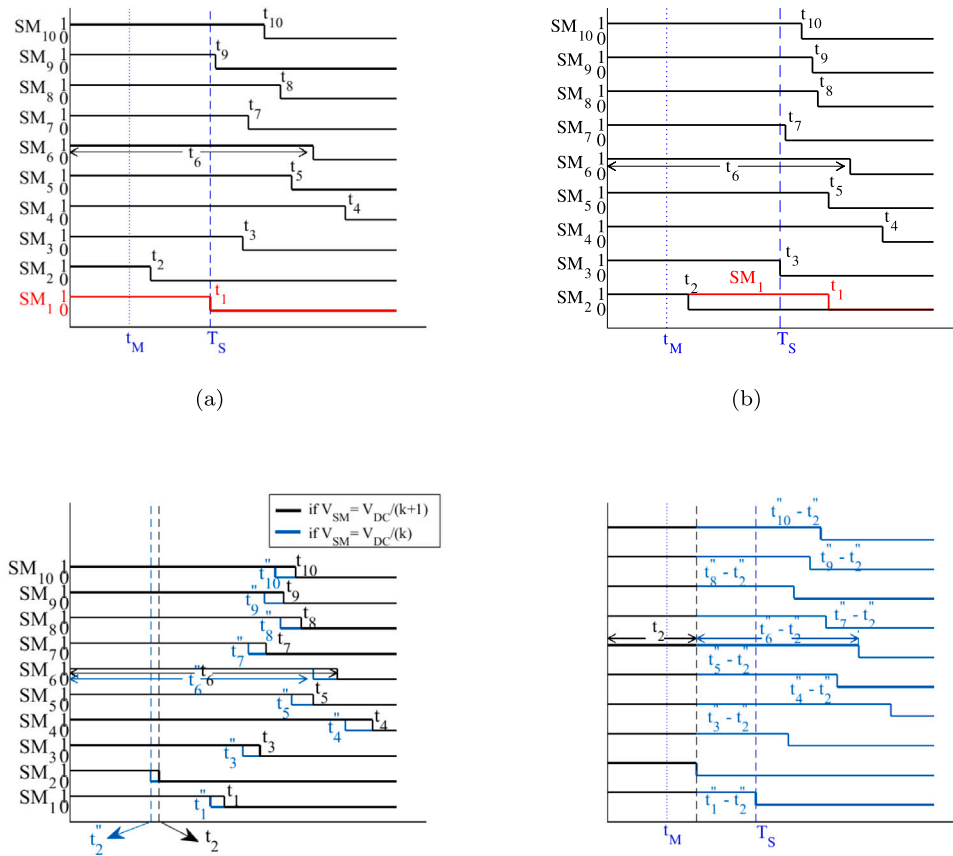


Fig. 2. Operating cycle of an arm of MMC with (a) FL-ARS; (b) SRS; and (c) LS-ARS.

repeat these trials to obtain results with acceptable accuracy, following the rule of conducting 10,000 trials. Additionally, t_M denotes the mission time, ranging from 0 to a specified time interval (30 years in this paper) with specific time steps (0.05 years in this study). In each trial, all SMs (SM_1, SM_2, SM_3, \dots) will have random operational intervals (t_1, t_2, t_3, \dots), respectively obtained from (11). Subsequently, the mission time is compared with the random operational interval of each SM, indicated by the marker \times . Each marker \times shown in Fig. 3 is achieved through the repetition of these trials (number of simulations) at that specific time.

This paper assesses an MMC with the characteristics outlined in Table 1 across various redundancy strategies. The configuration includes a minimum required number of SMs in each arm, denoted as $N_{min} = 9$. The base failure rates for the capacitor and IGBT are provided in Table 1. To account for voltage stress and other factors, the equations from [33], initially derived from MIL-HDBK (detailed in the appendix) [7], are implemented. The methodology for applying MCS to the MMC with different redundancy schemes is further elaborated below.

3.1. FL-ARS MCS

Each arm is configured with 10 SMs to assess the MMC with FL-ARS. The assumption is made that the minimum required number of SMs per arm is $N_{min} = 9$, and $N_{red} = 1$ represents the number of redundant SMs in each arm. The operational cycle of an arm utilizing FL-ARS is illustrated in Fig. 2(a).

In Fig. 2(a), the FL-ARS involves the operation of all n SMs, where only 9 out of 10 SMs are necessary for an arm to succeed. In this stochastic trial, at failure time (T_s), the second failure occurs, and T_s is equal to t_1 of SM_1 . Consequently, if mission time (t_M) is less than T_s , it is considered a successful mission; otherwise, it is deemed

Table 1

MMC characteristics and failure rates.

Symbols	Item	Value
N_{min}	Minimum number of SMs	9
V_{dc}	Pole-to-pole DC voltage	17 kV
S_{MMC}	Rated power	10 MVA
V_{IGBT}	Rated IGBT Voltage	3300 V
k_{max}	Capacitors voltage ripple	10%
S_f	Safety factor of IGBT	0.6
C_{SM}	SM capacitance	3.3 mF
f_{sw}	Switching frequency	313 Hz
N_{red}	Redundant per arm	1
IGBT	FF450R33T3E3(Infineon)	-
Capacitor	DKTFM1*#B3367(AVX)	-
$\lambda_{base-IGBT}$	IGBT base failure rate (MIL)	100 FIT [13]
$\lambda_{base-Cap}$	DC capacitor base failure rate (MIL)	100 FIT [13]

a failed mission. This experiment should be repeated, and the total number of successes (or failures) divided by the total number of trials yields the success (or failure) probability, as depicted in Fig. 3(a). This representation demonstrates that the applied methodology of FL-ARS MCS output with 1000 simulations aligns with the output results of analytical Eqs. (2) used for calculating the reliability of MMC with FL-ARS. Note that 1000 trials are selected to show the sporadic distribution of trials. With a higher number of trials, the MCS will exactly match the analytical outputs.

3.2. SRS MCS

In the case of the MMC arm employing SRS, the same number of SMs is utilized. The operating cycle of an arm with SRS is presented in Fig. 2(b). As illustrated, the number of operating SMs equals N_{min} , and the redundant SM (SM_1) remains in idle mode. In this stochastic trial,

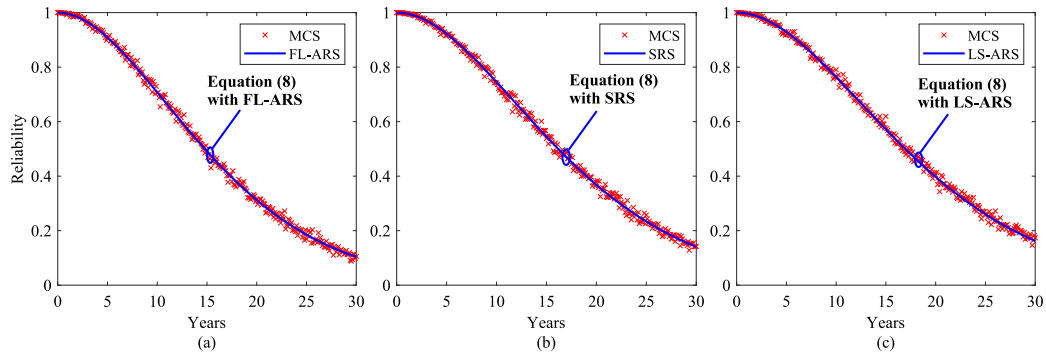


Fig. 3. MMC reliability applying analytical and MCS methods (1000 trials) for (a) FL-ARS; (b) SRS; and (c) LS-ARS.

the first failure occurs at t_2 (in SM_2), prompting the redundant SM_1 to start operating at t_2 . Consequently, at least nine operating SMs are required for the arm to succeed. However, the second failure occurs in SM_3 at t_3 , leading to the arm being considered failed beyond that time. Therefore, in this trial, T_s is equal to t_3 , and if t_M is less than T_s , that trial is counted as a success. As previously mentioned, this trial should be repeated. The ratio between the number of successful missions and the total number of trials yields the success probability, as shown in Fig. 3(b). The results presented in Fig. 3(b) validate the effectiveness of applying the SRS MCS methodology, as the analytical and MCS (1000 trials) outputs align.

3.3. LS-ARS MCS

Fig. 2(c) illustrates the operational cycle of an arm in the MMC employing LS-ARS. In LS-ARS, the number of operating SMs includes the redundant SM, and unlike FL-ARS and SRS, all SMs share the load. Consequently, the voltage stress is lower than both SRS and FL-ARS. However, in LS-ARS, the voltage across operating SMs in healthy conditions increases after each SM failure, leading to higher voltage stress over time. This factor is crucial to consider. As shown in Fig. 2(c) on the left side, if the voltage across each SM is $V_{SM} = \frac{V_{dc}}{N_{min} + N_{fed}}$, the voltage stress is lower than the case where the voltage across each SM is equal to $V_{SM} = \frac{V_{dc}}{N_{min}}$. Therefore, in this stochastic trial, the operational time of SMs in the former case (t_1, t_2, \dots, t_{10}) will be higher than in the latter case ($t_1'', t_2'', \dots, t_{10}''$).

After calculating the first step, the second step for evaluating the MCS of an arm under LS-ARS is presented in Fig. 2(c) on the right-hand side. At time 0, all the SMs are operational and share the load. When at t_2 , SM_2 fails, the remaining SMs operate with higher voltage stress. Hence, the remaining SMs' lifetime reduction can be calculated, as shown in Fig. 2(c) on the right-hand side, such as for SM_6 where the operational lifetime is equal to $t_2 + (t_6'' - t_2)$. Then T_s is calculated, since at t_1 , SM_1 fails in this stochastic trial, $T_s = t_2 + (t_1'' - t_2)$. After obtaining the operation cycle of MMC under LS-ARS, t_M is compared with T_s .

3.4. Error assessment: MCS vs. Analytical methods

This section assesses the difference between MCS and analytical methods given by (13). The outcomes of this evaluation are visually depicted in Fig. 4, which indicates that if the number of trials exceeds 10,000, it can be inferred that the error between analytical and MCS results is approximately 1%, which can be neglected.

$$\text{Error}(\%) = \left| \frac{R_{\text{MMC-MCS}} - R_{\text{MMC-analytical}}}{R_{\text{MMC-analytical}}} \right| \times 100 \quad (13)$$

4. Implementation of MCS in grid specific applications

This section will explain how the MCS solves several problems where providing an analytical solution is challenging or unavailable in the literature.

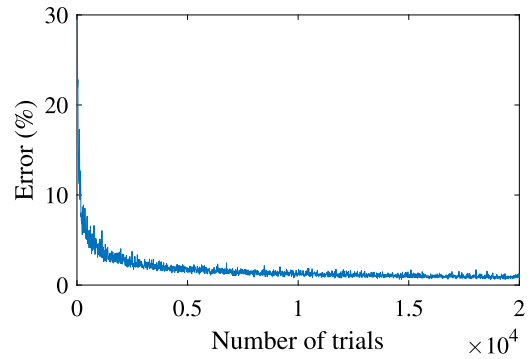


Fig. 4. Examining uncertainty of MCS results compared to analytical methods.

Table 2
Impact of redundancy schemes on the operational characteristics of the MMC.

	Voltage stress ^a	Operational losses ^b
FL-ARS	unchanged	unchanged
SRS	unchanged	unchanged
LS-ARS	changes	changes

^a Across IGBTs and capacitor bank.

^b Including conduction and switching losses.

4.1. Redundancy strategies for mission profile method

Conventional reliability evaluation methods for MMCs have analytical solutions when considering diverse redundancy strategies and applying MIL methods. The mission profile methods struggled to accommodate the complexity of different redundancy strategies beyond FL-ARS. Specifically, the mission profile method restricted evaluation to FL-ARS due to analytical constraints, leaving the reliability of MMCs with SRS and LS-ARS unaddressed. This gap in methodology hindered a comprehensive assessment of MMC reliability under varying operating conditions. To achieve this, the applicability of the MCS is assessed through FL-ARS, and the MMC's reliability is assessed without redundancy. Then, the MCS outputs for FL-ARS and without redundancy are compared with existing analytical equations (Eq. (2)) to validate the MCS's effectiveness in applying the mission profile method. Then, the MCS is extended for SRS and LS-ARS, where no analytical approach is provided.

Considering the MMC with the given characteristic in Table 1 [9, 12,25,34]. The impact of redundancy selectors on the operational characteristics of the MMC is summarized in Table 2.

It can be observed that under LS-ARS, the MMC needs to be reevaluated and modeled for $N_{min} + 1$ SMs in an arm after each SM failure. This is because the voltage stress across the remaining SMs and the operational losses will change after every failure.

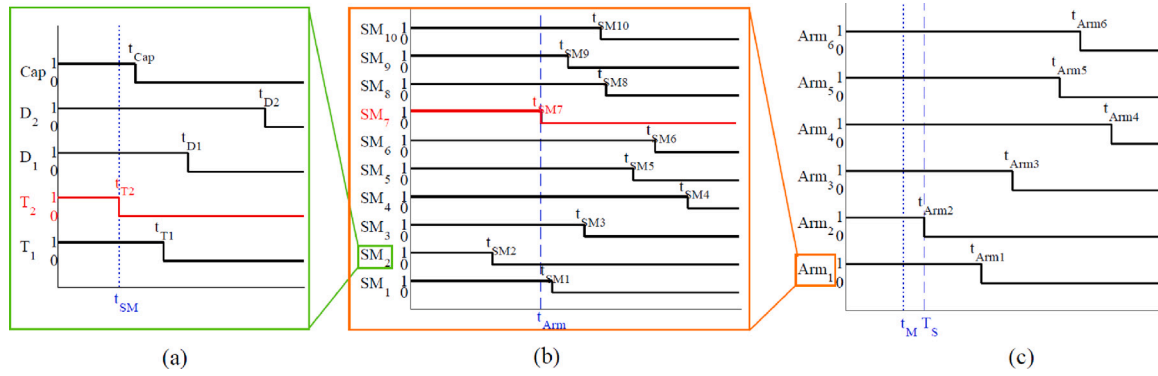


Fig. 5. Operating cycle of MMC with FL-ARS applying mission profile method at (a) SM, (b) Arm, and (c) MMC levels.

Table 3
Shape and Scale Factor parameters [12].

		T_1	T_2	D_1	D_2	Cap
$n=N_{min}$	η	5.1e3	110.4	3.1e3	5.5e3	147.3
	β	3.38	3.15	3.43	3.37	58.1
$n=N_{min}+N_{red}$	η	5.2e3	117.1	3.2e3	5.6e3	309.1
	β	3.36	3.15	3.38	3.37	42.2

In this study, two conditions are considered for an arm’s operation after the 1st SM failure:

1. When the arm is operating with $N_{min} + N_{red}$ SMs (including redundant SMs).
2. When the arm is operating with N_{min} SMs (excluding redundancy effects).

It is important to note that if there are more than one redundant SM ($N_{red} > 1$) in each arm, the reevaluation process needs to be repeated for $N_{red} + 1$ iterations. This is because the characteristics of the MMC — such as voltage stress distribution and operational losses — change after each SM failure. To model the reliability of MMC under LS-ARS and using the mission profile method, and since we have only one redundant SM, the system is modeled two times for LS-ARS. The lower row of Table 3 is added for healthy conditions and when there is no SM failure under LS-ARS. However, if one SM fails and needs to be bypassed, the voltage and characteristics of the system should be adopted accordingly, and therefore, the upper row of Table 3 is obtained. If one redundant SM is used, the output parameters improve because the voltage stress decreases across all the SMs validated in Table 3. To evaluate the system-level reliability of the MMC, these numbers should be converted into failure probability density function as well as reliability outputs as follows:

$$\begin{cases} f(t) = \frac{\beta}{\eta} (\frac{t}{\eta})^{\beta-1} e^{-(\frac{t}{\eta})^\beta} \\ R(t) = 1 - \int_0^t f(t) dt = e^{-(\frac{t}{\eta})^\beta} \end{cases} \quad (14)$$

where $f(t)$ is the failure probability density function, and $R(t)$ is the reliability of the components. Within the structure of the HB-SM, there are five components, including two IGBTs (T_1 and T_2), two body diodes for semiconductors (D_1 and D_2), and a capacitor bank (Cap). The successful operation of the SM requires that all these components remain healthy, as expressed by Eq. (15).

$$R_{SM}(t) = \prod R_k(t), k = T_1, T_2, D_1, D_2, Cap \quad (15)$$

The methodology of applying MCS for the mission profile method in the case of FL-ARS at arm level is presented in Fig. 5. As shown in Fig. 5(a), by applying Eq. (12) using the data in Table 3, each component that fails faster (in this case T_2), it is considered as the lifetime

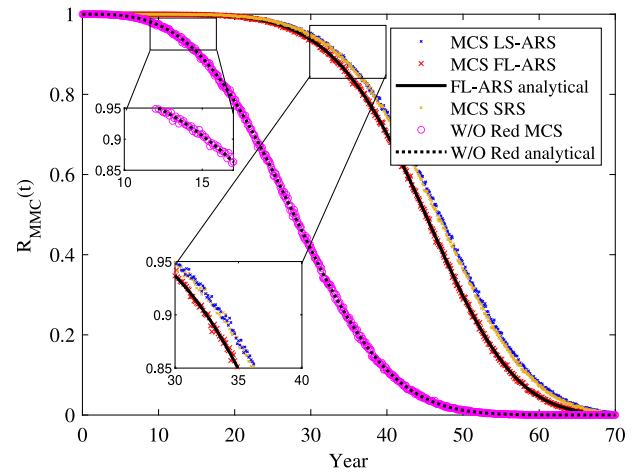


Fig. 6. Examining uncertainty of MCS results (10,000 trials) compared to analytical methods.

of that SM. Then, assuming that FL-ARS is the arm-level redundancy type shown in Fig. 5(b), where there are 10 SMs, the second failure (in this case, SM_7) is the lifetime of that arm, and the same strategy for the MMC shown in Fig. 5(c) where t_M is compared with T_s to estimate the reliability of the MMC.

In Fig. 6, the reliability of the MMC using the mission profile method with different redundancy strategies is presented by applying MCS. The analytical equations for the MMC without redundancy (dashed-black line) and FL-ARS (solid-black line) are available to validate the MCS’s effectiveness. Analytical equations for LS-ARS and SRS that apply the mission profile method are unaddressed due to mathematical challenges. However, by applying the MCS technique, the reliability of the MMC can be estimated. Besides the validation by analytical equations for FL-ARS and without redundancy, note that in the MIL method, the superiority of the redundancy strategies is consequently LS-ARS, SRS, and FL-ARS. The same trend can be seen in the case of the mission profile MCS outputs.

4.2. Maintenance considering aging effects in HVDC

In practical systems, improving reliability also relies on strategies like maintenance and stocking spares. Maintenance ensures that a system meets required performance and reliability standards while stocking spares provides redundancy without automatic switching, similar to standby redundancy. Preventive maintenance minimizes the likelihood of failures by preemptively addressing wear-out and replacing the faulty parts on time. For instance, components are tested before commissioning in power systems to avoid initial debugging failures.

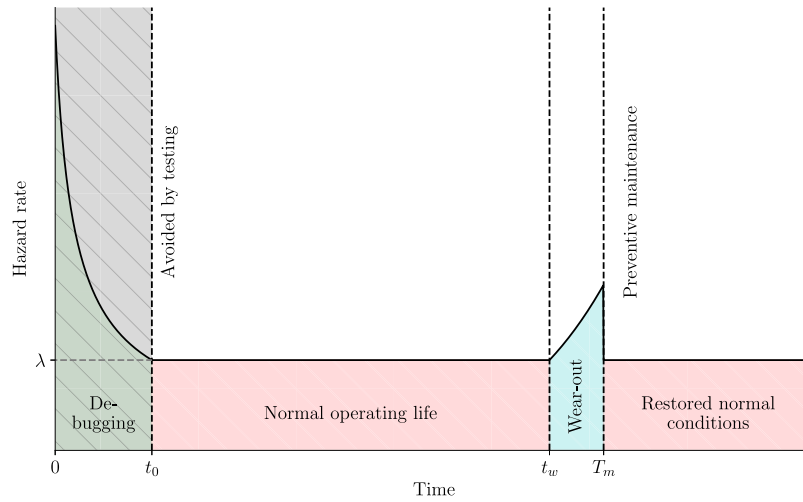


Fig. 7. System hazard rate considering wear-out failure and preventive maintenance.

This makes the hazard rate curve of periodically maintained assets discontinuous, as illustrated in Fig. 7.

Proper preventive maintenance can sustain high reliability over extended periods. This impacts the components' reliability function and mean time to failure (MTTF). With a maintenance interval T_m , the reliability function becomes discontinuous at each interval, as shown below:

$$R_{maintained}(t) = \begin{cases} R_x(t) & \text{if } 0 \leq t \leq T_m \\ R_x^i(T_m) \cdot R_x(t - iT_m) & \text{if } iT_m \leq t \leq (i + 1)T_m \end{cases} \quad (16)$$

$$MTTF_{maintained}(T_m) = \frac{\int_0^{T_m} R_x(t) dt}{1 - R_x(T_m)} \quad (17)$$

Here, $R_x^i(T_m)$ quantifies maintenance quality, ranging from 0 to 1, representing the success in restoring conditions to their original state $R_x(0)$. The exponent i accounts for the diminishing effectiveness of subsequent maintenance activities. While shorter maintenance intervals yield better performance, practical constraints like time and resources limit this choice.

The primary goal of maintenance is to reduce the probability of component or system failure by restoring normal operating conditions. This restoration directly influences the reliability modeling of components. The reliability function of a maintained MMC arm can be expressed as shown in (16). This model assumes a perfect periodic maintenance strategy, where the arm's reliability is fully restored to its initial state after each maintenance interval. This is depicted in Fig. 8, approximating the scenario where all SMs are inspected, and faulty SMs are replaced at regular intervals. However, only the replaced SMs are restored, not the entire arm. Despite this limitation, prior research [35] shows that the error introduced by this assumption is negligible ($\leq 0.1\%$) for typical redundancy levels, making it a reasonable simplification.

The introduced methods lack accuracy because they do not account for the system's mixed composition after maintenance. Specifically, the system consists of two groups of SMs: newly replaced SMs reset to their original "as-new" condition and operational SMs that have been in use and experienced wear. These groups have different failure probabilities, making the overall reliability more complex to model. Analytically, it is challenging to track the age and condition of each SM, compute their reliability, and aggregate this into a system-level measure. The interactions between new and aging SMs further complicate the analysis due to their evolving failure rates. As a result, traditional analytical methods struggle to capture the system's reliability under maintenance accurately. This limitation highlights the importance of simulation-based methods, which can better model such systems' dynamic and

stochastic nature. To assess the advantage of MCS over analytical equations, this part is designed to simulate real-life scenarios in the context of HVDC-MMC. In HVDC-MMC, operations and maintenance (O&M) are crucial for ensuring continuous functionality. MCS emerges as a potent solution. Through MCS, it becomes feasible to determine the optimal number of redundant SMs required in each arm, ensuring uninterrupted MMC operation. Moreover, the MCS methodology empowers us to estimate the annual frequency of maintenance, the number of faulty SMs, and how often staff intervention is needed.

This study adopts a dynamic preventive maintenance strategy based on the number of active redundant SMs in each arm of the system. For this purpose, the hot-reserved redundancy is detailed in Sections 2 A and 4 A. Also, for maintenance applications, aging effects are considered by applying a variable failure rate outlined in Section 3 (mission-profile Eq. (12)). In dynamic preventive maintenance, If there is only one active SM in an arm, replacement should be initiated after the first failure occurs in that specific arm. Maintenance should be performed after the second failure when two redundant SMs are in each arm. It is crucial to note that if faulty SMs are present in other arms, they should also be replaced. Similarly, when each arm contains three redundant SMs, maintenance should be conducted after the third failure, along with replacing faulty SMs in other arms. This maintenance approach ensures the operational continuity of the MMC, as there will always be at least a minimum number (N_{min}) of operational SMs available.

To enhance understanding of MCS working principles, Fig. 9 is included in this study. For simplicity, the figure considers an MMC configuration with six SMs in each arm, of which two are redundant. The results illustrated in Fig. 9 depict a trial scenario where the initial two failures occurred in arm 1, and arm six had previously encountered one failure (assuming no failures in other arms). Consequently, maintenance will be conducted shortly after the second failure in arm 1, replacing three faulty SMs with spare ones. It is essential to emphasize that this trial should be repeated multiple times to ensure statistically reliable results. Taking an example of the MMC in [34] with $N_{min} = 200$ and $N_{red} = 8$, the MCS results are presented in Fig. 10. The data (such as β and η for each component) used for this evaluation are all adopted from [34] given in Table 4. In Fig. 10(a), it is estimated that within 20 years of operation, eight times of maintenance is required for this particular MMC. Furthermore, Fig. 10(b) shows that the estimated number of potential SM failures that will be replaced with new SMs within the same period is around 233 SMs.

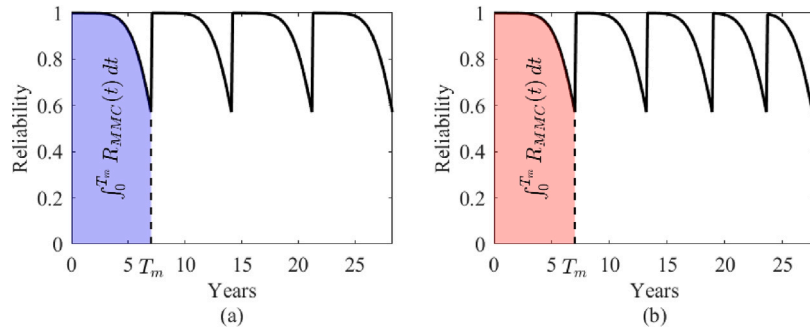


Fig. 8. Reliability function of the MMC considering (a) perfect periodic maintenance and (b) perfect preventive maintenance.

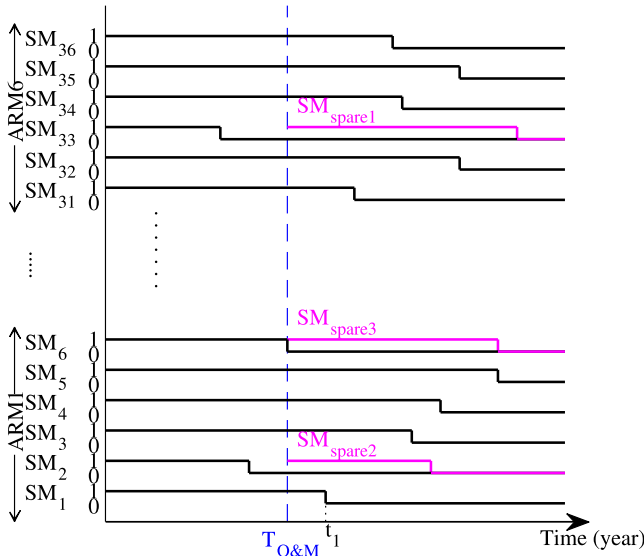


Fig. 9. Operating cycle of the MMC considering dynamic maintenance with 6 SMs in each arm, including two active redundant SMs ($N_{min} = 4, N_{red} = 2$).

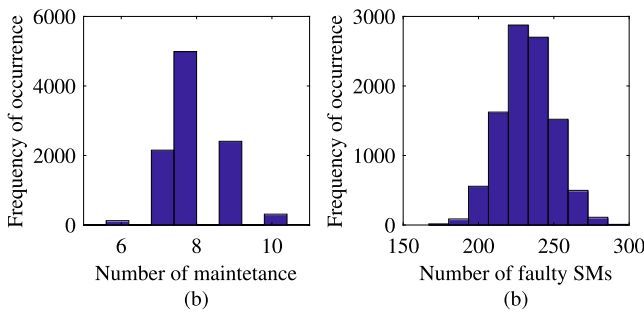


Fig. 10. MCS results (10,000 trials) for MMC with $N_{min} = 200$ and $N_{red} = 8$ (in 20 years) (a) the distribution of the estimated number of required O&M with $\mu = 8$ and $\sigma = 0.798$ (b) the distribution of the estimated number of SMs that will be replaced with $\mu = 233$ and $\sigma = 17.43$.

Table 4
Shape and Scale Factor parameters [34].

	T_1	T_2	D_1	D_2	Cap
η	836	37.2	495	378	63.6
β	2.58	2.42	2.57	2.54	14.7

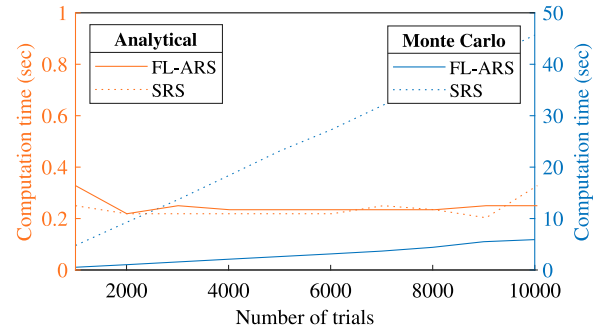


Fig. 11. Analytical and MCS computation time outputs for SRS and FL-ARS with varying trials.

Table 5

MCS computation time of SRS and FL-ARS for 10000 trials with different computer.

	Computer 1 (s)	Computer 2 (s)
SRS	45.672	27.89
FL-ARS	5.906	4.25

5. Computation time for Monte Carlo Simulation

Fig. 11 presents the computation time of MCS concerning the number of trials compared to the analytical solution for different redundancy strategies for the MMC. The results indicate that SRS has a higher computation time compared to FL-ARS, and this difference grows as the number of trials increases.

Fig. 12(a) shows that MCS has comparable computation time independent of N_{min} for FL-ARS and $N_{min} > 20$ for SRS. On the other hand, Fig. 12(b) shows that a higher level of redundancy results in increased MCS computation time. In this investigation, the computation time of MCS is compared on two different computers: Computer 1 (Laptop) and Computer 2 (PC). Computer 1, equipped with an 11th Gen Intel(R) Core(TM) i7-1185G7 @ 1.80 GHz, 16 GB RAM, and a 512 GB SSD, was compared against Computer 2, featuring an upgraded configuration with 12th Gen Intel(R) Core(TM) i5-12500 @ 3.00 GHz, 8 GB RAM, and a 512 GB SSD. The results unequivocally demonstrated that Computer 2 exhibited significantly improved performance in terms of computation time. The enhanced configuration of Computer 2, featuring a faster processor, enabled it to process the simulation 35% faster than Computer 1 (see Table 5).

6. Conclusion

This study proposes a detailed procedure for applying MCS with different redundancy strategies for MMC. The advantage of using MCS is demonstrated through its application in MMC maintenance, which poses challenges when analytical methods are employed. Also, the

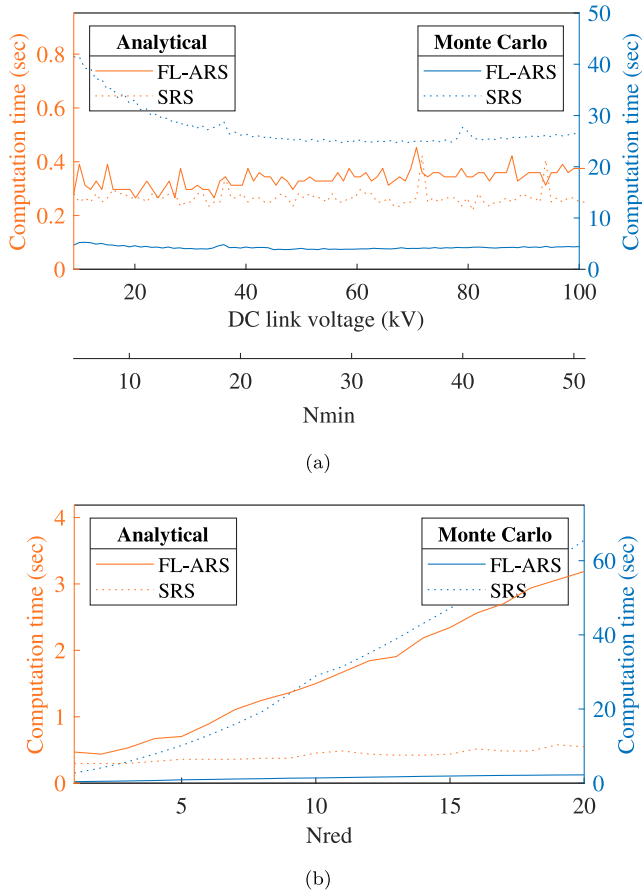


Fig. 12. Analytical and MCS computation time outputs for SRS and FL-ARS with (a) varying number of levels for 10000 trials, (b) varying number of redundancy ($N_{\min} = 51$).

reliability of the MMC with SRS and LS-ARS using the mission profile method, which was unaddressed, can be easily estimated by applying MCS. Additionally, the error in applying MCS is found to be less than 1% when the number of trials exceeds 10,000. MCS with FL-ARS took significantly lower computation time than SRS, particularly for more trials. For example, for 10,000 trials, it took approximately 45 s for SRS while only about 6 s for FL-ARS with $N_{\min} = 9$. It is interesting to observe that MCS for MMC with more SMs has comparable computation time, particularly when $N > 20$. For example, it still takes approximately 6 s for FL-ARS with 10 times higher SMs ($N_{\min} = 50$ for 10,000 trials). While an increase in redundancy results in a higher computation time, particularly for SRS. Overall, the proposed MCS approach provides a valuable tool for analyzing the performance of MMC systems. It can help engineers optimize the reliability-based design by digitizing such systems and plan application-dependent preventive maintenance, which is impossible with analytical equations.

CRedit authorship contribution statement

Miad Ahmadi: Writing – review & editing, Writing – original draft, Visualization, Validation, Methodology, Investigation, Formal analysis, Conceptualization. **Aditya Shekhar:** Validation, Supervision. **Pavol Bauer:** Resources, Funding acquisition.

Declaration of competing interest

The authors declare that they have no known competing financial interests or personal relationships that could have appeared to influence the work reported in this paper.

Appendix. MIL

In Tables A.6 and A.7, the failure rate of capacitors and IGBTs by applying the methodology in MIL-HDBK is given, respectively.

Table A.6

MIL equations for estimating failure rate of capacitor.

$$\lambda_{\text{MIL-Cap}} = \lambda_{\text{base-Cap}} \pi_T \pi_V \pi_{\text{SR}} \pi_Q \pi_E \pi_C$$

$$\pi_C = (C)^{0.09}$$

$$\pi_V = \left[\frac{V_{\text{applied}}}{0.6 \times V_{\text{rated}}} \right]^5 + 1$$

$$\pi_T = \exp \left[\frac{-0.15}{8.617 \times 10^{-3}} \left(\frac{1}{T_j + 273} - \frac{1}{298} \right) \right]$$

$$\pi_{\text{SR}} = 0.1, \pi_Q = 10, \pi_E = 1, \lambda_{\text{base-Cap}} = 100 \text{ FIT}$$

Table A.7

MIL equations for estimating failure rate of IGBT.

$$\lambda_{\text{MIL-IGBT}} = \lambda_{\text{base-IGBT}} \pi_T \pi_S \pi_A \pi_R \pi_E$$

$$\pi_S = 0.045 \times \exp \left[3.1 \frac{V_{\text{applied}}}{V_{\text{rated}}} \right]$$

$$\pi_T = \exp \left[-114 \times \left(\frac{V_{\text{rated}}}{T_j + 273} - \frac{1}{298} \right) \right]$$

$$\pi_A = 0.7, \pi_R = 1, \pi_E = 6, \lambda_{\text{base-IGBT}} = 100 \text{ FIT}$$

In which T_a is the capacitor ambient temperature, T_j is the IGBT junction temperature, C is the capacitance in μF , and π_x is different factors affecting the components failure rates specified in [7].

Data availability

Data will be made available on request.

References

- [1] Nazmul Huda AS, Živanović R. Study effect of components availability on distribution system reliability through multilevel Monte Carlo method. *IEEE Trans Ind Inform* 2019;15(6):3133–42. <http://dx.doi.org/10.1109/TII.2018.2877822>.
- [2] Sangwongwanich A, Blaabjerg F. Monte Carlo simulation with incremental damage for reliability assessment of power electronics. *IEEE Trans Power Electron* 2021;36(7).
- [3] Wang H, Liserre M, Blaabjerg F. Toward reliable power electronics: Challenges, design tools, and opportunities. *IEEE Ind Electron Mag* 2013;7(2):17–26. <http://dx.doi.org/10.1109/MIE.2013.2252958>.
- [4] Ahmadi M, Bertinato A, Boussaad I. Reliability analysis of the bus-bar systems in multiterminal HVDC systems. In: 2021 23rd European conference on power electronics and applications. 2021, p. P.1–P.10. <http://dx.doi.org/10.23919/EPE21ECCEEurope50061.2021.9570467>.
- [5] Ahmadi M, Shekhar A, Bauer P. Reconfigurability, modularity and redundancy trade-offs for grid connected power electronic systems. In: 2022 IEEE 20th international power electronics and motion control conference. 2022, p. 35–41. <http://dx.doi.org/10.1109/PEMC51159.2022.9962889>.
- [6] Huang H, Mawby PA. A lifetime estimation technique for voltage source inverters. *IEEE Trans Power Electron* 2013;28(8):4113–9. <http://dx.doi.org/10.1109/TPEL.2012.2229472>.
- [7] Reliability prediction of electronic equipment: MIL-HDBK-217D. Military standardization handbook, Department of Defense; 1983, URL <https://books.google.nl/books?id=CYSvEwEACAAJ>.
- [8] Shahidrad N, Niroomand M, Hooshmand R-A. Investigation of PV power plant structures based on Monte Carlo reliability and economic analysis. *IEEE J Photovolt* 2018;8(3).
- [9] Wang L, Xu J, Wang G, Zhang Z. Lifetime estimation of IGBT modules for MMC-HVDC application. *Microelectron Reliab* 2018;82:90–9. <https://doi.org/10.1016/j.microrel.2018.01.009>.
- [10] Jirutitijaroen P, Singh C. Comparison of simulation methods for power system reliability indexes and their distributions. *IEEE Trans Power Syst* 2008;23(2):486–93. <http://dx.doi.org/10.1109/TPWRS.2008.919425>.
- [11] Billinton R, Allan RN. Reliability evaluation of engineering systems: concepts and techniques. 1992.
- [12] Ahmadi M, Kardan F, Shekhar A, Bauer P. Reliability assessment of modular multilevel converters: A comparative study of MIL and mission profile methods. In: 13th international conference on integrated power electronics systems. 2024.
- [13] Tu P, Yang S, Wang P. Reliability- and cost-based redundancy design for modular multilevel converter. *IEEE Trans Ind Electron* 2019;66(3):2333–42. <http://dx.doi.org/10.1109/TIE.2018.2793263>.

- [14] Feng F, Yu J, Yang Z, Dai W, Zhao X, Kamel S, Wang J, Fu G. Dynamic preventive maintenance strategy for MMC considering multi-term thermal cycles. *Int J Electr Power Energy Syst* 2020;116:105560. <http://dx.doi.org/10.1016/j.ijepes.2019.105560>.
- [15] Ahmadi M, Shekhar A, Bauer P. Mixed redundancy strategy for modular multilevel converters in high-power applications. *IEEE Open J Ind Electron Soc* 2024;5:535–46. <http://dx.doi.org/10.1109/OJIES.2024.3415007>.
- [16] Zhou D, Wang H, Blaabjerg F. Mission profile based system-level reliability analysis of DC/DC converters for a backup power application. *IEEE Trans Power Electron* 2018;33(9).
- [17] Liu W, Xu Y. Reliability modeling of MMC-based flexible interconnection controller considering the uncertainty of current loading. *Microsyst Technol* 2019;25:905–16.
- [18] Zhang T, Chen X, Yu Z, Zhu X, Shi D. A Monte Carlo simulation approach to evaluate service capacities of EV charging and battery swapping stations. *IEEE Trans Ind Informatics* 2018;14(9):3914–23. <http://dx.doi.org/10.1109/TII.2018.2796498>.
- [19] Zhang Y, Wang H, Wang Z, Blaabjerg F, Saeedifard M. Mission profile-based system-level reliability prediction method for modular multilevel converters. *IEEE Trans Power Electron* 2020;35(7):6916–30. <http://dx.doi.org/10.1109/TPEL.2019.2957826>.
- [20] Novak M, Sangwongwanich A, Blaabjerg F. Monte Carlo based reliability estimation methods in power electronics. In: *IEEE 21st workshop on control and modeling for power electronics*. 2020.
- [21] Júnior PR, Cupertino AF, Mendonça GA, Pereira HA. On lifetime evaluation of medium-voltage drives based on modular multilevel converter. *IET Electr Power Appl* 2019;13(10):1453–61. <http://dx.doi.org/10.1049/iet-epa.2018.5897>.
- [22] Farias JVM, Cupertino AF, Ferreira Vd, Pereira HA, Seleme SI, Teodorescu R. Reliability-oriented design of modular multilevel converters for medium-voltage STATCOM. *IEEE Trans Ind Electron* 2020;67(8):6206–14. <http://dx.doi.org/10.1109/TIE.2019.2937050>.
- [23] Zhang Y, Wang H, Wang Z, Blaabjerg F, Saeedifard M. Mission profile-based system-level reliability prediction method for modular multilevel converters. *IEEE Trans Power Electron* 2020;35(7):6916–30. <http://dx.doi.org/10.1109/TPEL.2019.2957826>.
- [24] Billinton R, Karki R. Application of Monte Carlo simulation to generating system well-being analysis. *IEEE Trans Power Syst* 1999;14(3):1172–7. <http://dx.doi.org/10.1109/59.780954>.
- [25] Gatla RK, Chen W, Zhu G, Zeng D, Nirudi R. Lifetime estimation of modular cascaded H-bridge MLPVI for grid-connected PV systems considering mission profile. *Microelectron Reliab* 2018;88–90:1051–6.
- [26] Liu H, Ma K, Qin Z, Loh PC, Blaabjerg F. Lifetime estimation of MMC for offshore wind power HVDC application. *IEEE J Emerg Sel Top Power Electron* 2016;4(2):504–11. <http://dx.doi.org/10.1109/JESTPE.2015.2477109>.
- [27] Xie X, Li H, McDonald A, Tan H, Wu Y, Yang T, Yang W. Reliability modeling and analysis of hybrid MMCs under different redundancy schemes. *IEEE Trans Power Deliv* 2021;36(3):1390–400. <http://dx.doi.org/10.1109/TPWRD.2020.3008281>.
- [28] Abeynayake G, Li G, Joseph T, Liang J, Ming W. Reliability and cost-oriented analysis, comparison and selection of multi-level MVdc converters. *IEEE Trans Power Deliv* 2021;36(6):3945–55. <http://dx.doi.org/10.1109/TPWRD.2021.3051531>.
- [29] Ahmadi M, Shekhar A, Bauer P. Switch voltage rating selection considering cost-oriented redundancy and modularity-based trade-offs in modular multilevel converter. *IEEE Trans Power Deliv* 2023;1–12. <http://dx.doi.org/10.1109/TPWRD.2023.3263270>.
- [30] Xu J, Jing H, Zhao C. Reliability modeling of MMCs considering correlations of the requisite and redundant submodules. *IEEE Trans Power Deliv* 2018;33(3):1213–22. <http://dx.doi.org/10.1109/TPWRD.2017.2757607>.
- [31] Huber JE, Kolar JW. Optimum number of cascaded cells for high-power medium-voltage AC-DC converters. *IEEE J Emerg Sel Top Power Electron* 2017;5(1):213–32. <http://dx.doi.org/10.1109/JESTPE.2016.2605702>.
- [32] Ahmadi M, Shekhar A, Bauer P. Impact of the various components consideration on choosing optimal redundancy strategy in MMC. In: *2022 IEEE 20th international power electronics and motion control conference*. 2022, p. 21–6. <http://dx.doi.org/10.1109/PEMC51159.2022.9962860>.
- [33] Guo J, Wang X, Liang J, Pang H, Gonçalves J. Reliability modeling and evaluation of MMCs under different redundancy schemes. *IEEE Trans Power Deliv* 2018;33(5).
- [34] Xu J, Wang L, Li Y, Zhang Z, Wang G, Hong C. A unified MMC reliability evaluation based on physics-of-failure and SM lifetime correlation. *Int J Electr Power Energy Syst* 2019;106:158–68. <http://dx.doi.org/10.1016/j.ijepes.2018.09.044>.
- [35] Yu P, Fu W, Wang L, Zhou Z, Wang G, Zhang Z. Reliability-centered maintenance for modular multilevel converter in HVDC transmission application. *IEEE J Emerg Sel Top Power Electron* 2020;9(3):3166–76.